Structural Engineering and Mechanics, *Vol. 70, No. 3 (2019) 289-301*
DOI: https://doi.org/10.12989/sem.2019.70.3.289

A new practical equivalent linear model for estimating seismic hysteretic energy demand of bilinear systems

Maryam Samimifar[1], Ali Massumi*[1] and Abdolreza S. Moghadam[2]

[1]*Department of Civil Engineering, Faculty of Engineering, Kharazmi University, Tehran, Iran*
[2]*Structural Engineering Research Center, International Institute of Earthquake Engineering and Seismology, Tehran, Iran*

(Received September 20, 2018, Revised February 22, 2019, Accepted February 24, 2019)

Abstract. Hysteretic energy is defined as energy dissipated through inelastic deformations during a ground motion by the system. It includes frequency content and duration of ground motion as two remarkable parameters, while these characteristics are not seen in displacement spectrum. Since maximum displacement individually cannot be the appropriate criterion for damage assessment, hysteretic energy has been evaluated in this research as a more comprehensive seismic demand parameter. An innovative methodology has been proposed to establish a new equivalent linear model to estimate hysteretic energy spectrum for bilinear SDOF models under two different sets of earthquake excitations. Error minimization has been defined in the space of equivalent linearization concept, which resulted in equivalent damping and equivalent period as representative parameters of the linear model. Nonlinear regression analysis was carried out for predicting these equivalent parameter as a function of ductility. The results also indicate differences between seismic demand characteristics of far-field and near-field ground motions, which are not identified by most of previous equations presented for predicting seismic energy. The main advantage of the proposed model is its independency on parameters related to earthquake and response characteristics, which has led to more efficiency as well as simplicity. The capability of providing a practical energy based seismic performance evaluation is another outstanding feature of the proposed model.

Keywords: linearization; hysteretic energy; seismic demand; equivalent period; equivalent damping; far-field; near-field

1. Introduction

The main objective of nonlinear seismic analysis is to predict the structure demands subjected to future probable ground motions more precisely (Fatahi *et al.* 2011). Due to existence of overstrength capacity and the capabilities of structures for dissipating input energy of the earthquakes, the seismic design codes allow the structures to experience inelastic deformations during the ground motions, while linear analyzes are utilized in the most cases in order to provide simplicity and applicability. In addition, the seismic rehabilitation standards of buildings use two general procedures for estimating target performance point of a building, that are equivalent linearization and displacement coefficients methods. Nowadays nonlinear time history analyzes are accessible by various computer programs along with different ground motion records as the inputs. However, high sensitivity of the results to the record characteristics, large number of model assumptions, and long time needed for analysis, has led to an attempt to achieve simplified approaches. Using an equivalent linear system with effective parameters to estimate maximum response of the nonlinear system is one of these techniques, which has been utilized in different researches usually with a focus on displacement spectra. In other words, the maximum displacement of a nonlinear SDOF system is estimated from a linear SDOF system with higher damping and lower stiffness. Equivalent linear parameters including damping and period, are called effective parameters.

Various methods have been developed by researchers to linearize nonlinear systems subjected to earthquake excitation. Secant period as the effective linear period has been used in most preliminary methods. Gulkan and Sozen (1974) found that the secant period and effective damping equations derived based on harmonic excitation lead to smaller maximum displacement response predictions compared to maximum inelastic earthquake response because of the large damping values. Incorporating shake table results of small-scale reinforced concrete frames in addition to simulation using the Takeda hysteretic model, Gulkan and Sozen (1974) developed a new effective damping equation as a function of ductility. Kowalsky (1994), also using the secant period as the effective linear period and the Takeda hysteretic model, presented another equation for effective damping. Secant period also has been used in Capacity Spectrum Method of ATC-40 (ATC 1996). By comparing linear and nonlinear velocity spectrum for a hysteretic SDOF model under seismic excitations, Iwan (1980) proposed two different equations for effective period and damping. Priestley *et al.* (1996) and Otani *et al.* (2000) are among other researchers, which developed equations for effective parameters as function of ductility and post yield stiffness ratio for different excited hysteretic

*Corresponding author, Professor
E-mail: massumi@khu.ac.ir

Copyright © 2019 Techno-Press, Ltd.

ISSN: 1225-4568 (Print), 1598-6217 (Online)

models. A new statistical approach with an optimization criterion has been used by Guyader and Iwan (2006) for calculating effective parameters of four hysteretic SDOF models subjected to a suite of earthquake records. The optimal point in two-dimensional parameter space of effective period and damping was taken as a point that minimizes the probability that error lies outside the engineering acceptability range. Ratio of the difference between linear system maximum displacement and inelastic system maximum displacement to the latter one has been considered as their simple error measure. They revealed that the ATC-40 (ATC 1996) equations are significantly unconservative and conservative respectively at high and low values of ductility. Oguzmert and Lui (2011) also presented equations for equivalent linear system parameters using a two-dimensional minimization technique for estimating inelastic seismic displacement demand of bilinear and degrading hysteretic SDOF models from elastic response spectra. They used root mean square averaged spectral error measure. Results show better prediction of inelastic displacement demand compared to other methods applied by most of other previous researchers for ductile systems with natural period between 0.3 to 3 seconds. In addition, Su *et al.* (2012) used particle swarm optimization technique in two-dimensional space of effective damping and period to obtain a linear system equivalent to the inelastic system in terms of displacement.

All these studies use almost different procedures for utilizing equivalent linearization methodology to obtain an equivalent linear system, which can predict seismic displacement demand of inelastic SDOFs. Browning *et al.* (2008) and Yaghmaei-sabegh *et al.* (2014) utilized this method to find maximum roof displacement of reinforced concrete frames subjected to earthquake records. They presented an optimized value and not equation for effective damping and period for the group of studied buildings located on high and moderate seismicity region.

Development in application of performance-based seismic design concepts is observed in the past few years, which has been resulted to a natural growth in the evaluation procedures of buildings (Fatahi *et al.* 2014). Contrary to both force-based and displacement-based design methods, energy-based design can directly consider the cumulative damage effect resulted from numerous inelastic cycles of the earthquake caused by deterioration of the hysteretic behavior of structure. In other words, different levels of structural damage are expected taking into account both the plastic deformation and cumulative energy absorption capacities of the main structural components during the earthquakes (Samimifar and Massumi 2018). In addition, seismic energy is a more comprehensive demand parameter, which can take into account force and displacement quantities. Considering these facts, many believe that energy-based methods will be the next generation of seismic design methods as well as performance based seismic evaluation methods of structures. Fajfar and Vidic (1994) are one of the first researchers investigated in this field. They developed an equation for estimating hysteretic energy (E_H) of bilinear SDOF systems subjected to five earthquake records. The equation relates E_H to several parameters including ductility reduction factor, spectral acceleration at fundamental period, and some of the records characteristics such as PGA, PGV and PGD. Then, Manferedi (2001) presented hysteretic energy of elasto-plastic SDOFs as a function of ductility, spectral acceleration, ductility reduction factor and equivalent number of cycles of the ground motion. In another study, E_H has been related to system's period, characteristics of the records (PGA, PGV, PGD) and time duration regardless of any response parameters by Riddell and Garcia (2001). Equation constants are dependent on the type of hysteretic model. The hysteric behavior is one of the most important factors affecting amount of hysteretic energy, as has been discussed and proven in some papers (Riddell and Garcia 2001, Decanini and Mollaioli 2001, Molazadeh and Saffari 2018).

Developed equation by Arroyo and Ordaz (2007) for E_H spectrum is based on a parameter related to number of cycles in addition to velocity and pseudo-acceleration spectrums at the shifted period, which is the main difference of their method compared to previous ones. Moreover, the investigations (Fajfar and Vidic 1994, Manfredi 2001, Kunnath and Chai 2004) show that for a specific type of hysteretic behavior, the ratio of hysteretic energy demand to input energy (E_I) is just depended on ductility ratio. Cheng *et al.* (2015) proposed an improved equivalent velocity spectrum for estimating elastic input energy as a parameter with potential of predicting seismic structural response. In another research, Mezgebo (2015) using average and standard deviation through each class of selected far-field earthquake records on different soil types, presented equations to be adopted to general shapes for normalized input energy spectrum and the spectrum of E_H/E_I ratio for four different hysteretic models. Normalization has done by a new defined velocity index as the product of Cumulative Absolute Velocity and Peak Ground Velocity of ground motion. Similarly, in order to overcome the shortcomings of common energy spectrums, Dindar *et al.* (2015) expressed E_I and E_H design spectrums in the form of a simple equation for elasto-plastic SDOF systems considering both far- and near-field earthquake records. It was concluded that in short period region, the type of hysteretic model used does not have much effect on the spectrum of energy while more significant differences are observed in the region of post spectrum peak periods when model is changes. Sun *et al.* (2017) are the other researchers, which use regression analysis to extract a normalized cumulative hysteretic energy spectrum. In line with estimating energy demand, the relationship between PGA and PGV has been established.

It was originally stated that the linear energy spectrum, regardless of its damping component, could be a logical approximation of the energy spectrum for nonlinear systems (Housner 1956), which was not approved by other researchers due to inadequate precision, especially in higher ductility levels (Uang and Bertero 1990). As previously described, due to importance of the issue many researches have been conducted to present equations for estimating E_H and E_I of nonlinear systems and their ratio separately. Due

to non-comprehensive initial parameters considered in those studies, such as limited number of records, or use of special basic assumptions, there is not enough assurance to generalize the results. Investigations show that, even in cases where the quantity of inputs appears to be sufficient, the proposed spectra can be significantly different in similar cases. On the other hand, most of the equations presented for estimating hysteric energy spectra are very complicated and depend on many parameters including earthquake and system characteristics, which, although in some cases, have the proper precision but do not have the required efficiency and capacity required for engineering codes.

From the practical point of view, many methods for evaluating the performance of structures use linear equivalent SDOF systems with different definitions according to what the purpose of that specific research is. In energy based methods, researchers (Enderami *et al.* 2014, Ambrisi and Mezzi 2015, Manoukas *et al.* 2014, Wang *et al.* 2018) were looking for an appropriate demand spectrum to be matched with resulting capacity curve. Although those definitions for demand spectrums are called "energy demand" but are not directly correlated with the values of the seismic energy obtained from mathematical integration of the equation of motion. In other words, the advantages and superiority of seismic energy spectrums to current response spectrums is not taken into account for these proposed types of energy demand.

There are damage indices, which defined based on displacement and energy demands (Massumi and Gholami 2016). Since the maximum displacement, individually, cannot be an appropriate criterion for damage assessment (Monavari and Massumi 2012), hysteretic energy has been evaluated in this research as a more comprehensive seismic demand parameter. With regard to the above literature, to overcome the deficiencies and complexities of the previous equations, a new equivalent linearization method has been used in this study, which can estimate seismic hysteretic energy of nonlinear hysteretic SDOF systems at different levels of ductility. Two sets of far- and near-field earthquake records has been utilized as the inputs of time history analysis. Philosophy of the procedure and its steps to derive equivalent linear SDOF model has been described in details first. In the next step, the effects of some parameters on the results have been discussed. Moreover, nonlinear regression analysis used to extract correlation coefficients to present classified equations for the equivalent parameters. Main advantage of the proposed model is its independency on parameters related to earthquake and response characteristics in its appearance, while incorporated frequency content and duration of earthquake simultaneously in itself. In fact, the simplicity as well as the applicability seems to be the most significant features of this new model, which has been obtained using error optimization in the space of equivalent linearization concept.

2. Basics and components of seismic energy

The equation of motion for an inelastic SDOF system subjected to a ground motion is given by

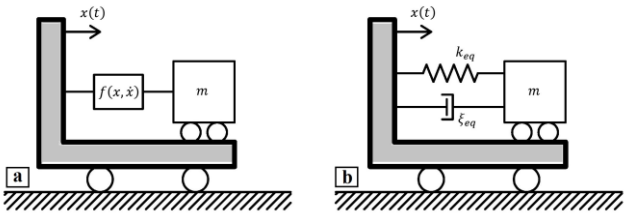

Fig. 1(a) Nonlinear, and (b) equivalent linear, single-degree-of-freedom structural models

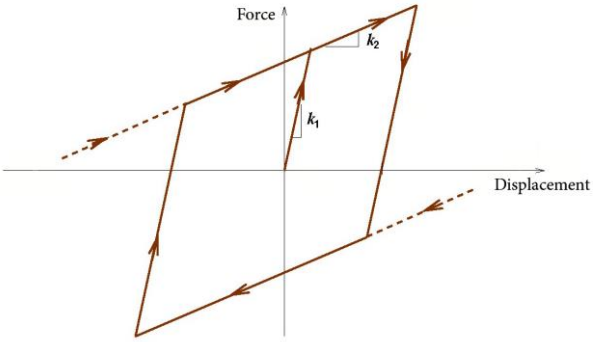

Fig. 2 Bilinear model

$$m\ddot{u} + c\dot{u} + f_s = -m\ddot{u}_g \tag{1}$$

where m is the mass of the system, c is the damping coefficient; f_s is the restoring force, $\ddot{u}_g$ is the ground acceleration, and $\ddot{u}$, $\dot{u}$, u are the relative acceleration, velocity, and displacement of the system with respect to the ground, respectively.

The energy balance equation for an SDOF system is derived directly by integrating the equation of motion with respect to the relative displacement response (Kalkan and Kunnath 2007).

$$\int m\ddot{u}\,du + \int c\dot{u}\,du + \int f_s\,du = -\int m\ddot{u}_g\,du \tag{2}$$

$$\int m\ddot{u}\dot{u}\,dt + \int c\dot{u}\dot{u}\,dt + \int f_s\dot{u}\,dt = -\int m\ddot{u}_g\dot{u}\,dt \tag{3}$$

Kinetic (E_K), damping (E_D) and hysteretic (E_H) energies represent the energy components of the system, which respectively compose the terms on the left hand side of Eq. (3). The right hand side of the equation represents total Input energy (E_I) imposed to the system. The hysteretic energy term also includes elastic strain energy (E_S) and plastic strain energy (E_P) caused by elastic and inelastic deformation the structure undergoes during the earthquake respectively. Thus,

$$E_K + E_D + E_H = E_I \;\; ; \;\; E_H = E_S + E_P \tag{4}$$

Kinetic energy vanishes during reversal of system velocity (Kalkan and Kunnath 2007). Therefore, this component becomes zero when vibration of the structure stops. Hysteretic energy could inflict permanent damage to the structure unless otherwise dissipated through some mechanisms.

3. Methodology to derive equivalent linear model

There are many uncertainties in ground motion event, and consequently the parameters associated with it. As mentioned in the previous section, many factors can affect both seismic input and hysteretic energies of structures, which can be classified in three general categories: nonlinear system characteristics, system response parameters, and earthquake characteristics. This research, concentrating on the main characteristics of nonlinear system and finding the relationship between linear and nonlinear energy spectrums by error minimization in the space of equivalent linearization concept, eliminates other parameters such as system responses and earthquake characteristics in energy estimation equation. In other words, since in this study hysteretic energy spectrum is estimated based on corresponding linear energy spectrum, both include the earthquake characteristics equally, and independent of the response parameters, thus more simple and practical results are made from an engineering point of view.

Based on our extensive investigations on energy spectrums, it is concluded that the hysteretic energy of a nonlinear SDOF system with natural period of T_0 can be estimated using the calculated damping energy for a linear system with a larger viscose damping and shifted period comparing to the original system. In fact, in addition to considering damping increase, shifted period is used as the natural period of equivalent linear system. The period shifting coefficient in this paper is henceforth called beta (β). Since both linear and corresponding nonlinear energy spectra are derived from a given earthquake and consequently incorporated frequency content and duration of earthquake similarly, there is no need to directly consider some parameters such as number of earthquake cycles in the new model. In other words, the main advantage of the proposed model is its independency on parameters related to earthquake and response characteristics, which has led to more efficiency.

Fig. 1 illustrates a nonlinear SDOF model with restoring force of $f(x,\dot{x})$ dependent on hysteresis behavior and an equivalent linear model with increased fraction of critical damping, ξ_{eq}, and shifted period, T_{eq}, subjected to a ground motion excitation, $\ddot{u}_g(t)$. The equation of motion for these models are respectively as follows;

$$(a)\ \ddot{x} + \left(\frac{4\pi\xi_0}{T_0}\right)\dot{x} + f(x,\dot{x}) = -\ddot{u}_g(t) \tag{5}$$

$$(b)\ \ddot{x} + \left(\frac{4\pi\xi_{eq}}{T_{eq}}\right)\dot{x} + \left(\frac{2\pi}{T_{eq}}\right)^2 x = -\ddot{u}_g(t) \tag{6}$$

As described, the purpose of current study is to find an equivalent linear model to estimate hysteretic energy demand of Bi-Linear Hysteretic (BLH) systems using nonlinear time history analyses results. The force-displacement relationship in BLH systems is illustrated in Fig. 2. The methodology utilizes the far-field and near-field record sets presented in FEMA P695 (2009) for nonlinear dynamic analysis. These sets respectively include twenty-two records (44 individual components) and twenty-eight records (56 individual components) selected from the PEER NGA database. For each record, Tables 1-2 summarizes the magnitude, year, and name of the event, as well as site characteristics and epicentral distances.

To implement the method in the form of an algorithm, it is necessary to calculate linear damping spectra for viscous damping ratios from 5 to 50% at intervals of 5%. The next step at this stage is to calculate the hysteretic energy spectra for bilinear hysteretic SDOF models in ductility range of 1.2 to 6 ductility with a regular increment of 0.2. The post yield slope ratio of the nonlinear models is considered equal to 0, 5%, and 10% respectively as the three most commonly used cases.

After calculating all the desired spectra for each record, an algorithm with the following steps has been coded to be run for each Far- and Near- set of records individually.

Step 1. Considering the shape of energy spectrums and the investigations carried out in the field, it is concluded that selected range for initial period of system should be classified to smaller groups in order to get more accurate results. Therefore, the initial period range of 0.1 to 4 seconds has been consecutively grouped in to six subgroups as T_0 = (0.1-0.5), (0.6-1), (1.1-1.5), (1.6-2), (2.1-3), and (3.1-4) in second. At the first step one of the mentioned group should be selected to run the following steps for it.

Table 1 Summary of earthquakes of the far-field record set (FEMA P695 2009)

No.	Earthquake				NEHRP Site Class	Site-Source Distance (km)	
	M	Year	Name	Station		Epicentral	Closest to Plane
1	6.7	1994	Northridge	Beverly Hills – Mulhol	D	13.3	17.2
2	6.7	1994	Northridge	Canyon Country-WLC	D	26.5	12.4
3	7.1	1999	Duzce, Turkey	Bolu	D	41.3	12.0
4	7.1	1999	Hector Mine	Hector	C	26.5	11.7
5	6.5	1979	Imperial Valley	Delta	D	33.7	22.0
6	6.5	1979	Imperial Valley	El Centro Array #11	D	29.4	12.5
7	6.9	1995	Kobe, Japan	Nishi-Akashi	C	8.7	7.1
8	6.9	1995	Kobe, Japan	Shin-Osaka	D	46.0	19.2
9	7.5	1999	Kocaeli, Turkey	Duzce	D	98.2	15.4
10	7.5	1999	Kocaeli, Turkey	Arcelik	C	53.7	13.5
11	7.3	1992	Landers	Yermo Fire Station	D	86.0	23.6
12	7.3	1992	Landers	Coolwater	D	82.1	19.7
13	6.9	1989	Loma Prieta	Capitola	D	9.8	15.2
14	6.9	1989	Loma Prieta	Gilroy Array #3	D	31.4	12.8
15	7.4	1990	Manjil, Iran	Abbar	C	40.4	12.6
16	6.5	1987	Superstition Hills	El Centro Imp. Co.	D	35.8	18.2
17	6.5	1987	Superstition Hills	Poe Road (temp)	D	11.2	11.2
18	7.0	1992	Cape Mendocino	Rio Dell Overpass	D	22.7	14.3
19	7.6	1999	Chi-Chi, Taiwan	CHY101	D	32.0	10.0
20	7.6	1999	Chi-Chi, Taiwan	TCU045	C	77.5	26.0
21	6.6	1971	San Fernando	Hollywood Stor	D	39.5	22.8
22	6.5	1976	Friuli, Italy	Tolmezzo	C	20.2	15.8

Table 2 Summary of earthquakes of the near-field record set (FEMA P695 2009)

No.	Earthquake				NEHRP Site Class	Site-Source Distance (km)	
	M	Year	Name	Station		Epicentral	Closest to Plane
1	6.5	1979	Imperial Valley-06	El Centro Array #6	D	27.5	1.4
2	6.5	1979	Imperial Valley-06	El Centro Array #7	D	27.6	0.6
3	6.9	1980	Irpinia, Italy-01	Sturno	B	30.4	10.8
4	6.5	1987	Superstition Hills-02	Parachute Test Site	D	16.0	1.0
5	6.9	1989	Loma Prieta	Saratoga - Aloha	C	27.2	8.5
6	6.7	1992	Erzican, Turkey	Erzincan	D	9.0	4.4
7	7.0	1992	Cape Mendocino	Petrolia	C	4.5	8.2
8	7.3	1992	Landers	Lucerne	C	44.0	2.2
9	6.7	1994	Northridge-01	Rinaldi Receiving Sta	D	10.9	6.5
10	6.7	1994	Northridge-01	Sylmar - Olive View	C	16.8	5.3
11	7.5	1999	Kocaeli, Turkey	Izmit	B	5.3	7.2
12	7.6	1999	Chi-Chi, Taiwan	TCU065	D	26.7	0.6
13	7.6	1999	Chi-Chi, Taiwan	TCU102	C	45.6	1.5
14	7.1	1999	Duzce, Turkey	Duzce	D	1.6	6.6
15	6.8	6.8	Gazli, USSR	Karakyr	C	12.8	5.5
16	6.5	1979	Imperial Valley-06	Bonds Corner	D	6.2	2.7
17	6.5	1979	Imperial Valley-06	Chihuahua	D	18.9	7.3
18	6.8	1985	Nahanni, Canada	Site 1	C	6.8	9.6
19	6.8	1985	Nahanni, Canada	Site 2	C	6.5	4.9
20	6.9	1989	Loma Prieta	BRAN	C	9.0	10.7
21	6.9	1989	Loma Prieta	Corralitos	C	7.2	3.9
22	7.0	1992	Cape Mendocino	Cape Mendocino	C	10.4	7.0
23	6.7	1994	Northridge-01	LA - Sepulveda VA	C	8.5	8.4
24	6.7	1994	Northridge-01	Northridge - Saticoy	D	3.4	12.1
25	7.5	1999	Kocaeli, Turkey	Yarimca	D	19.3	4.8
26	7.6	1999	Chi-Chi, Taiwan	TCU067	C	28.7	0.6
27	7.6	1999	Chi-Chi, Taiwan	TCU084	C	8.9	11.2
28	7.9	2002	Denali, Alaska	TAPS Pump Sta. #10	C	7.0	8.9

Step 2. Based on selected group of natural periods, the beta coefficient larger than 0.1 have been used with an increment of 0.1 to calculate equivalent period, T_{eq}.

Step 3. A constant target ductility is selected ($1 < \mu \leq 6$). Constant increments of 0.2 are used when the loops come back to the current step. (counter: $r = 1 \dots m$)

Step 4. An input value from the assumed range is assigned to the equivalent damping ratio, ξ_{eq}. (counter: $j = 1 \dots q$)

Step 5. Beta is the next parameter that should be selected from the specified range of second step. (counter: $i = 1 \dots p$)

Step 6. Depending on which set of records is being investigated, one of the 44 (far-field) or 56 (near-field) earthquake records is picked. (counter: $k = 1 \dots s$)

Step 7. According to selected class of initial periods, an input value for T_0 is selected. Value of 0.1 is used as the period increment when the loops come back to the current step. (counter: $l = 1 \dots n$)

After this step, two independent series of commands (substeps) should be executed in parallel, which named as 7.1 and 7.2.

Step 7.1.1. The equivalent period is calculated;

$$T_{eq} = \beta T_0 \tag{7}$$

Step 7.1.2. Damping energy is calculated for the linear SDOF system with natural period of T_{eq} and viscous damping ratio of ξ_{eq}, $E_D(\xi_{eq}, T_{eq})$.

Step 7.2.1. The nonlinear BLH SDOF model parameters are selected (post yield slope ratio and linear viscous damping of $\xi_0 = 5\%$).

Step 7.2.2. Hysteretic energy is calculated for the bilinear SDOF system with post yield ratio of α, natural period of T_0 and damping ratio of ξ_0, $E_H(\xi_0, T_0, BLH, \alpha, \mu)$.

Step 8. If $l \leq n$, should be returned to Step 7, otherwise, Step 9 is the next to continue.

Step 9. If $k \leq s$, should be returned to Step 6, otherwise, Step 10 is the next to continue.

Step 10. The root mean square averaged spectral error function (ε) should be computed at this step as follows;

$$\varepsilon\left(\left(\frac{T_{eq}}{T_0}\right)_i, \left(\xi_{eq}\right)_j\right) = \sqrt{\frac{1}{n}\sum_{l=1}^{n}\left[\frac{\sum_{k=1}^{s}\left(\left(E_D\left(\left(\frac{T_{eq}}{T_0}\right)_i, \left(\xi_{eq}\right)_j\right)\right)_{lk} - (E_H)_{lk}\right)}{\sum_{k=1}^{s}(E_H)_{lk}}\right]^2} \tag{8}$$

Step 11. If $i \leq p$, should be returned to Step 5, otherwise, Step 12 is the next to continue.

Step 12. Since equivalent damping is considered constant during each loop, the minimum of error has to be search over the space of equivalent periods. For the specified equivalent damping, the minimum error corresponds to the optimum equivalent period of defined model. Actually at this step, an optimized pair of equivalent period ratio and damping $\left(T_{eq}/T_0, \xi_{eq}\right)$ is obtained.

Step 13. If $j \leq q$, should be returned to Step 4, otherwise, Step 14 is the next to continue.

Step 14. If $r \leq t$, should be returned to Step 3, otherwise, Step 1 is the next to select another class of periods and repeat all the steps of algorithm.

Step 15. If the whole process was done for all six classes of first step, the algorithm is finished.

4. Equivalent linear parameters

Considering constant values for equivalent damping in the range of 5 to 50 percent, the optimum ratio of equivalent to initial period resulted from the far- and near-field sets of records are respectively shown in Fig. 3 and Fig. 4 as a function of ductility for BLH systems with 10% post yield

(a) $0.1 \leq T < 0.5$

(b) $0.5 \leq T \leq 1.0$

(c) $1.0 < T \leq 1.5$

(d) $1.5 < T \leq 2.0$

(e) $2.0 < T \leq 3.0$

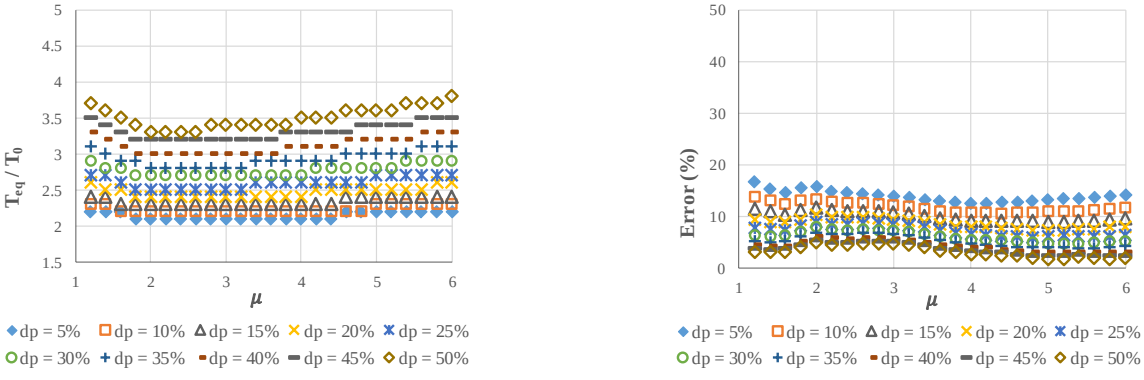

(f) $3.0 < T \leq 4.0$

Fig. 3(a)-(f); Optimized ratio of equivalent to initial period of BLH systems with post yield slope ratio of 10% and corresponding minimized error for far-field record set; (dp: equivalent damping)

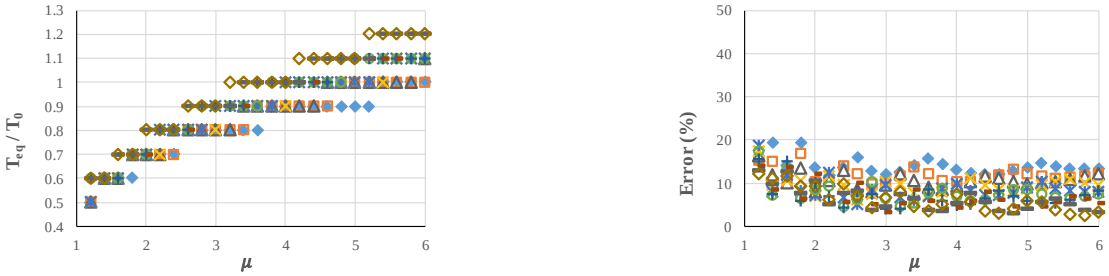

(a) $0.1 \leq T \leq 0.5$

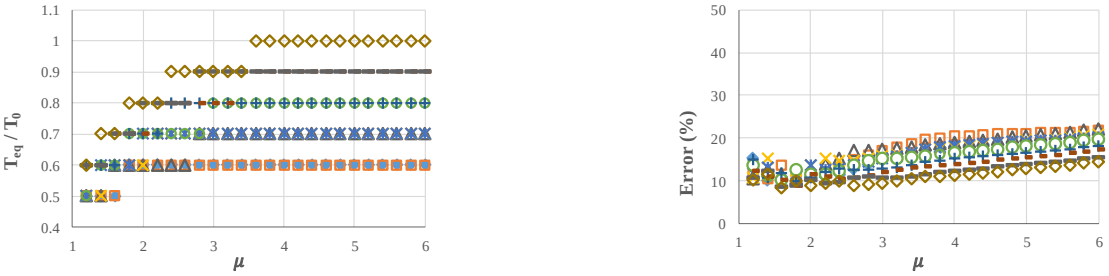

(b) $0.5 < T \leq 1.0$

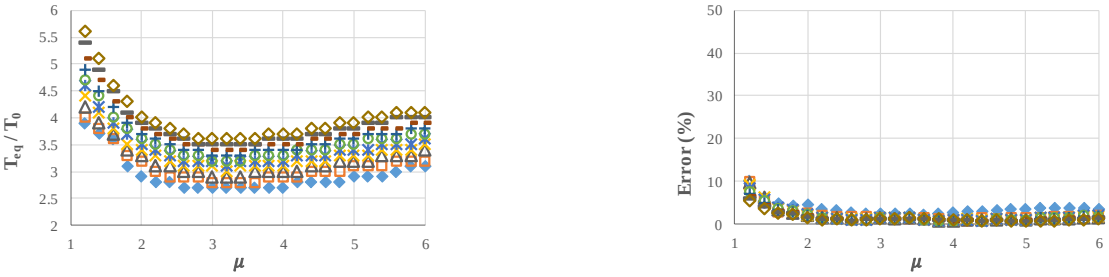

(c) $1.0 < T \leq 1.5$

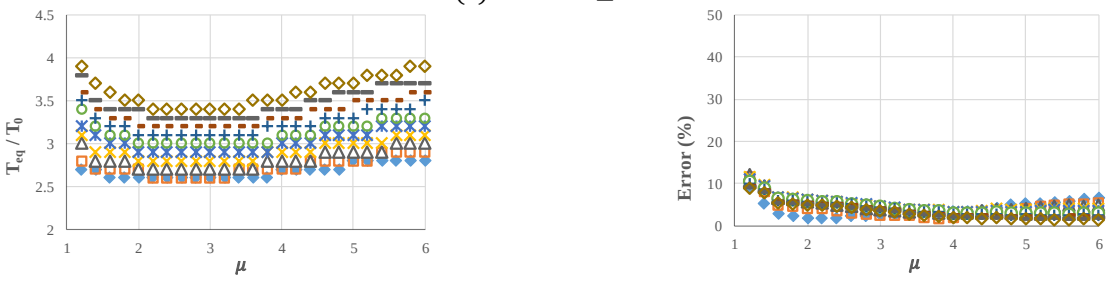

(d) $1.5 < T \leq 2.0$

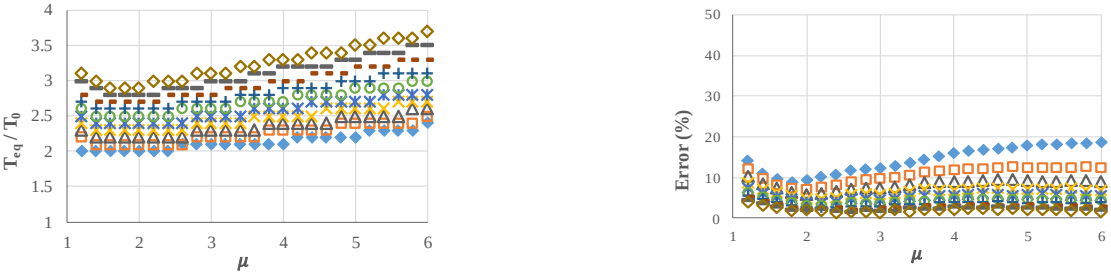

(e) $2.0 < T \leq 3.0$

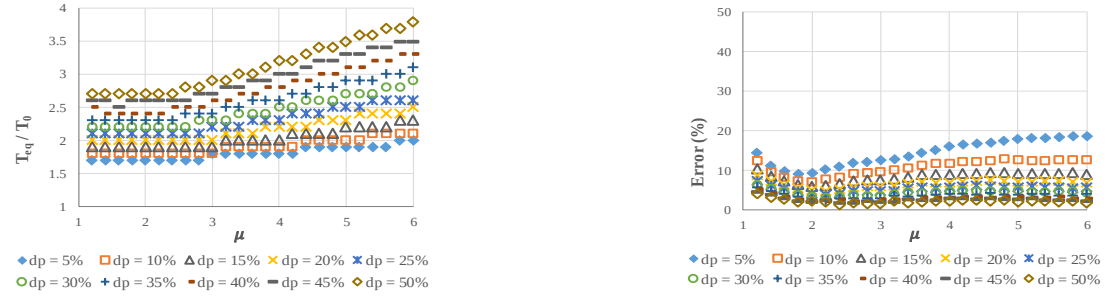

(f) $3.0 < T \leq 4.0$

Fig. 4(a)-(f); Optimized ratio of equivalent to initial period of BLH systems with post yield slope ratio of 10% and corresponding minimized error for near-field record set; (dp: equivalent damping)

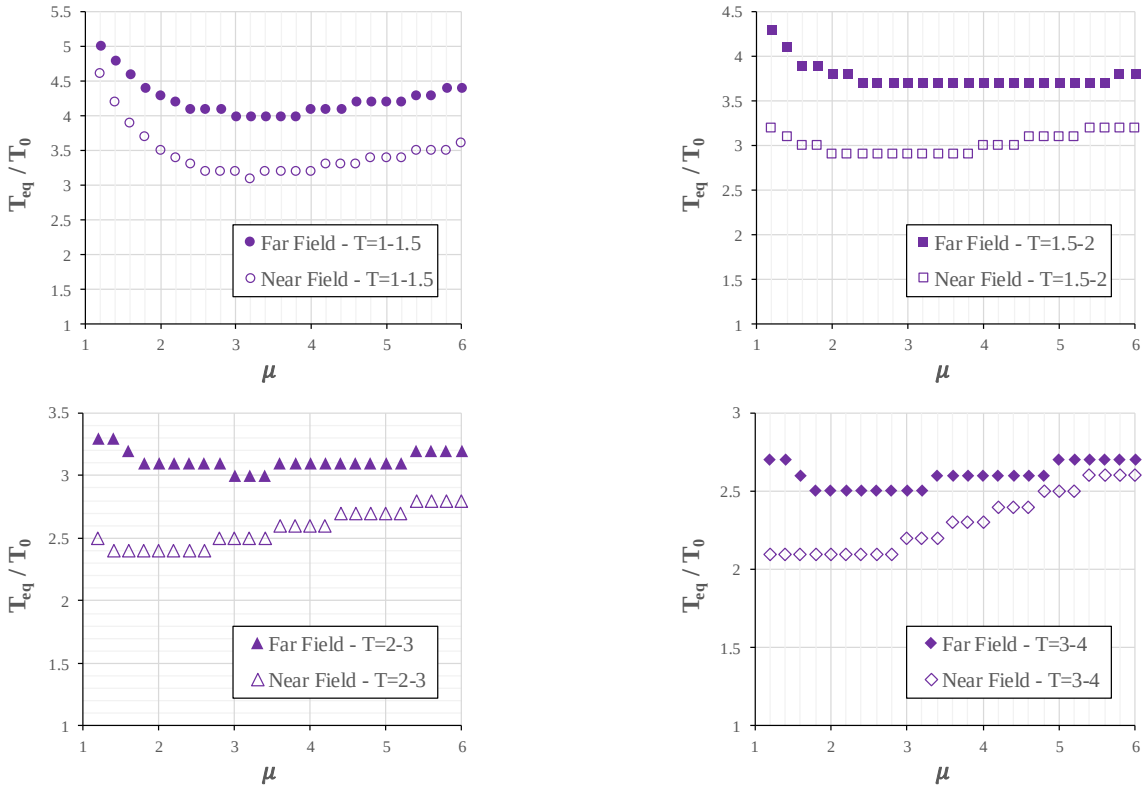

Fig. 5 Comparing results of far- and near-field sets of record for a constant equivalent damping of 25% and BLH systems with post yield slope ratio of 10%

slope ratio. It is observed that for a given value of ductility, increasing equivalent damping will also increase the ratio of equivalent to initial period, while the corresponding error measure decreases. Consequently, the minimum error occurs at the largest equivalent damping. It has been determined that from an engineering design point of view adesirable range of error values is between 0 and 20% (Guyader and Iwan 2006). Almost all current error values are existed in this desired range as can be seen in Figs. 3 and 4.

Investigating the energy spectrum of the far- and near-field earthquake records shows that, on average, spectral energy values in short period region increase with period until the maximum value is reached whereas, a decreasing trend for energy is generally observed with increasing periods thereafter. The peak values of the hysteretic energy spectrums of the far- and near-field sets of records occurs approximately at periods (here called T_p) of 0.5 and 1 seconds respectively. As a result, the trend obtained for the optimum equivalent period ratios is different depending on whether the period in question is greater than T_p or less than that. Generally speaking, for periods smaller than T_p, optimum equivalent period ratios increase with ductility, while for longer periods this is the opposite and dominant trend is descending.

For initial periods larger than T_p, results extracted from the far-field set indicate that, generally, the optimum ratio of equivalent to initial period decreases as the ductility increases. Of course, when initial periods are moving toward larger quantities, slope of the graphs is reducing so that in larger ductilities, the equivalent period ratio can be considered to be approximately equal to a constant value (almost like a straight line). The results obtained from the near-field records (in the range of periods larger than T_p) also show a decrease in the ratio of equivalent period with increasing ductility when smaller periods groups are intended, while in the range of larger periods, with increasing ductility, the rate of decline gradually decreases as far as for periods greater than 2 seconds, ascending trend can be observed in corresponding charts.

The graphs depicted in the Figs. 3-4 also indicate a decrease in the ratio of equivalent period with increase of initial period. For nonlinear SDOF oscillators, increasing initial period will generally decrease absorbed hysteretic energy as a response amplitude, which makes it possible to achieve the desired response by applying smaller coefficient (β) within the linear damping spectrum compared to when systems with smaller periods are intended.

It can be observed that for a specified system and a given equivalent damping, the optimum equivalent period ratio obtained based on the far-field set of records is larger than the corresponding value obtained from the near-field set. Assuming a BLH system with post yield slope ratio of10% as an example, the results of far and near set of earthquake records for a constant equivalent damping of 25% are compared in Fig. 5. It is worth noting that based on Figs. 3-4, this conclusion is confirmed for all the studied cases.

Since hysteretic energy is one of the components of the seismic input energy, their ratio (E_H/E_I) has been

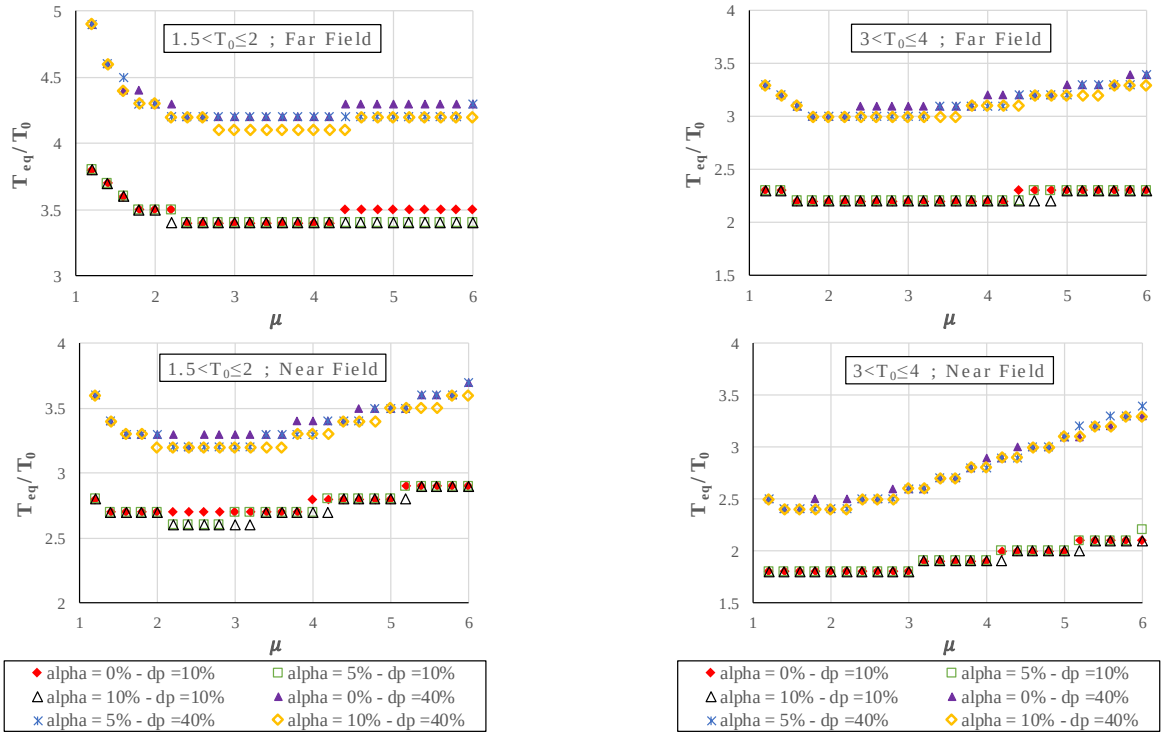

Fig. 6 Comparing the optimized ratio of equivalent to initial period of BLH systems with post yield slope ratio of 0%, 5% and 10% for two different constant equivalent dampings (dp) taking into account both far- and near-field sets of record

calculated for all the specified cases herein. As expected, in the range of common structural systems period (up to 4 seconds), for a given value of ductility, the ratio of hysteretic to input energy, on average, is larger when near-field set of records is selected. Indeed, if the near-field earthquake records are considered, hysteric energy will be provided a larger contribution in input energy compared to far-field set of records. Therefore, assuming a constant value for ductility, it is necessary to apply a larger shift to the initial period of system over the linear damping energy spectrum in order to obtain desired value of the hysteretic energy as a far-field earthquake record is intended compared with a record of near-field.

Since three different values for the post yield stiffness ratio of the studied models are considered, the effect of this parameter on the responses is also evaluated. As a result, it is observed that in all cases, the post yield slope ratio variation from 0 to 10% does not significantly affect the values of the equivalent parameters. Fig. 6 compares the responses for different values of this parameter in some cases as examples.

As previously described, the proposed equivalent linear model for hysteretic energy estimation can be written as follows.

$$E_H^{inel}(BLH, \alpha, \mu, T_0, \xi_0) = E_D^{el}\left(T_{eq}, \xi_{eq}\right) \tag{9}$$

Three-variable nonlinear regression analysis has been utilized to provide the best fit to the datasets resulted from the proposed procedure for each of defined cases. The optimum values of T_{eq}/T_0 may be graphed as function of ductility for a constant value of ξ_{eq}. Observations upon many sets of optimal points revealed a relatively different trend in both the equivalent period and damping present for ductilities between 4.0 and 6.0 for far records set and also between 3.5 and 6.0 for near records set as initial period greater than T_p was intended. Optimal points are fitted with a rational function (ratio of two polynomials) for all cases. The equivalent parameters equations are presented separately for far- and near-field earthquake records. Constant coefficients in Eqs. (10)-(13) for the models with post yield slope ratios of 0%, 5% and 10% are shown in Tables 3-4.

The general form of the equations for far-field set of records is assumed to be

$$0.1 \le T_0 < 0.5 \Rightarrow$$

$$\frac{T_{eq}}{T_0} = \frac{10^2}{A\mu^3 + B\mu^2 + C\mu + D\xi_{eq} + E} \quad 1 < \mu \le 6 \tag{10}$$

$$0.5 \le T_0 \le 4.0 \Rightarrow$$

$$\begin{cases} \dfrac{T_{eq}}{T_0} = \dfrac{10^2}{A\mu^3 + B\mu^2 + C\mu + D\xi_{eq} + E} & 1 < \mu < 4 \\ \dfrac{T_{eq}}{T_0} = \dfrac{10^2}{F\mu + G\xi_{eq}^2 + H\xi_{eq} + I} & 4 \le \mu \le 6 \end{cases} \tag{11}$$

For near-field set of records the following general form is considered as well.

$$0.1 \le T_0 \le 1.0 \Rightarrow$$

$$\frac{T_{eq}}{T_0} = \frac{10^2}{A\mu^3 + B\mu^2 + C\mu + D\xi_{eq} + E} \quad 1 < \mu \le 6 \tag{12}$$

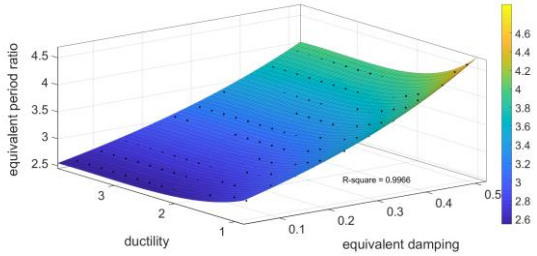

(a) $2 < T_0 \leq 3\ ;\ 1 < \mu < 4\ ;$ Far − Field Set

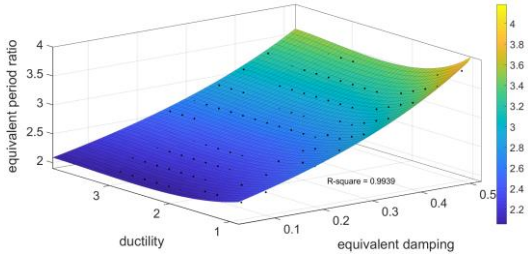

(b) $3 < T_0 \leq 4\ ;\ 1 < \mu < 4\ ;$ Far − Field Set

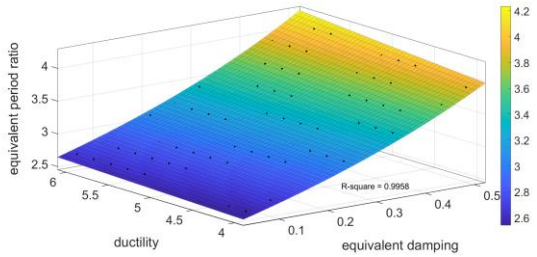

(c) $2 < T_0 \leq 3\ ;\ 4 \leq \mu \leq 6\ ;$ Far − Field Set

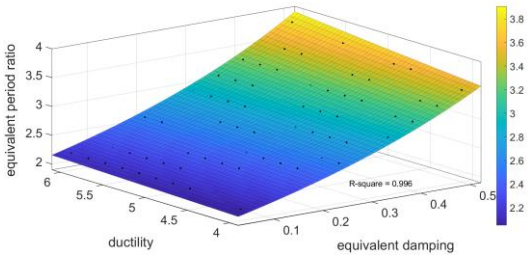

(d) $3 < T_0 \leq 4\ ;\ 4 \leq \mu \leq 6\ ;$ Far − Field Set

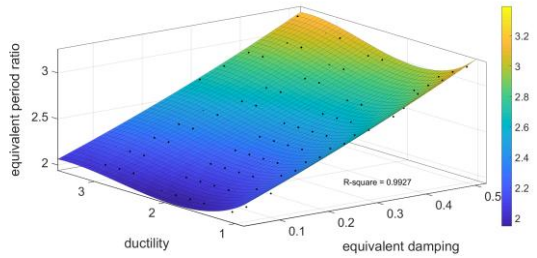

(e) $2 < T_0 \leq 3\ ;\ 1 < \mu < 3.5\ ;$ Near − Field Set

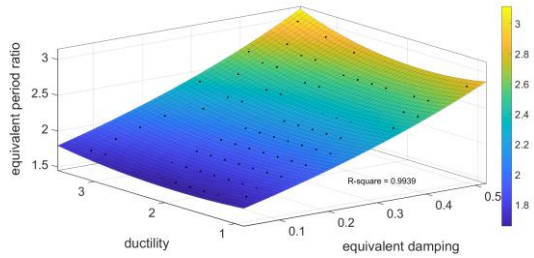

(f) $3 < T_0 \leq 4\ ;\ 1 < \mu < 3.5\ ;$ Near − Field Set

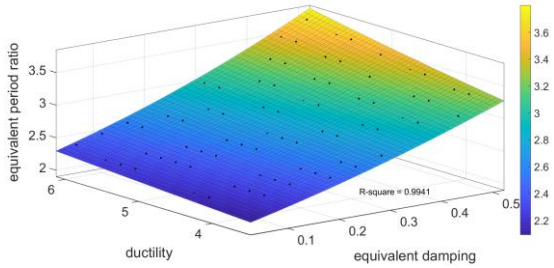

(g) $2 < T_0 \leq 3\ ;\ 3.5 \leq \mu \leq 6\ ;$ Near − Field Set

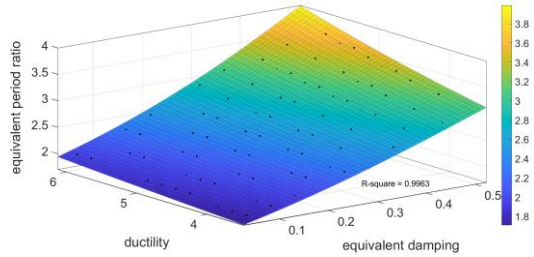

(h) $3 < T_0 \leq 4\ ;\ 3.6 \leq \mu \leq 6\ ;$ Near − Field Set

Fig. 7(a)-(h); Examples of optimum equivalent linear parameters (equivalent period ratio and equivalent damping) for BLH system with 10% of post yield slope ratio: discrete points and curve fit to data

$1.0 < T_0 \leq 4.0 \Rightarrow$

$$\begin{cases} \dfrac{T_{eq}}{T_0} = \dfrac{10^2(\xi_{eq} + A)}{B\mu^3 + C\mu^2 + D\mu + E\xi_{eq} + F} & 1 < \mu < 3.5 \\ \dfrac{T_{eq}}{T_0} = \dfrac{10^2}{G\mu + H\xi_{eq}^2 + I\xi_{eq} + J} & 3.5 \leq \mu \leq 6 \end{cases} \quad (13)$$

All data fitting is done by a nonlinear least squares approach that minimizes the absolute error difference between the optimal point and the analytical expression. The three dimensional fitted curves including eight different cases are illustrated in Fig. 7 as examples. R-square is the square of the correlation between the response values and the predicted response values, which can measure how successful the fit is in explaining the variation of the data statistically. It is also called the square of the multiple correlation coefficient. R-square can take on any value between 0 and 1, with a value closer to 1 indicating that a greater proportion of variance is accounted for by the model. It can be observed that R-square values are all about 0.99, which represents a great fit.

5. Conclusions

The energy based seismic evaluation (EBSE) methods are ensuring that structural capacity can meet the hysteretic energy demand of an earthquake. In the other words, the evaluation is satisfactory if the hysteretic energy demand of a system due to an earthquake can be dissipated through an

Table 3 Constant coefficients of equivalent linear parameters equations, Eqs. (10)-(11), the case of far-field record set

α	T_0	A	B	C	D	E	F	G	H	I
0%	$0.1 \le T < 0.5$	-1.164	16.49	-82.51	-19.28	254.8				
	$0.5 \le T \le 1$	0.232	-3.266	14.34	-15.43	5.232	-0.325	22.98	-35.43	30.92
	$1 < T \le 1.5$	0.095	-1.539	7.379	-14.89	17.00	-0.815	-2.863	-12.70	30.87
	$1.5 < T \le 2$	0.421	-4.067	12.88	-18.65	17.85	-0.118	0.376	-18.19	31.27
	$2 < T \le 3$	0.448	-4.158	12.46	-29.08	27.62	-0.932	6.632	-32.82	43.64
	$3 < T \le 4$	0.710	-6.154	16.86	-41.02	34.71	-1.070	13.28	-49.68	53.78
5%	$0.1 \le T < 0.5$	-1.121	16.61	-86.40	-25.05	260.7				
	$0.5 \le T \le 1$	0.142	-2.823	14.14	-15.30	5.025	-0.499	22.20	-34.65	32.04
	$1 < T \le 1.5$	0.047	-1.388	7.619	-14.81	16.59	-0.795	-5.477	-10.98	30.52
	$1.5 < T \le 2$	0.434	-4.139	13.10	-18.34	17.58	-0.221	0.490	-19.04	32.41
	$2 < T \le 3$	0.416	-3.936	12.17	-28.74	27.58	-0.846	6.253	-32.41	43.44
	$3 < T \le 4$	0.500	-4.812	14.50	-40.71	35.82	-1.082	11.70	-48.65	54.01
10%	$0.1 \le T < 0.5$	-1.261	18.39	-93.36	-27.78	267.2				
	$0.5 \le T \le 1$	0.195	-3.276	15.43	-15.47	4.193	-0.341	24.80	-36.87	32.23
	$1 < T \le 1.5$	0.043	-1.441	8.012	-14.88	16.25	-0.791	-5.139	-11.09	30.70
	$1.5 < T \le 2$	0.450	-4.302	13.63	-18.37	17.18	-0.204	-2.464	-16.91	32.20
	$2 < T \le 3$	0.385	-3.732	11.84	-28.77	27.74	-0.707	5.230	-31.56	42.99
	$3 < T \le 4$	0.452	-4.449	13.81	-40.16	36.00	-1.077	11.16	-48.17	54.29

Table 4 Constant coefficients of equivalent linear parameters equations, Eqs. (12)-(13), the case of near-field record set

α	T_0	A	B	C	D	E	F	G	H	I	J
0%	$0.1 \le T \le 0.5$	-1.231	17.51	-87.57	-40.90	272.5					
	$0.5 < T \le 1$	-1.252	17.20	-77.39	-118.3	287.4					
	$1 < T \le 1.5$	3.707	-2.218	5.596	27.05	-44.37	62.43	-0.903	19.64	-30.16	40.32
	$1.5 < T \le 2$	13.49	11.09	-96.17	265.9	-279.5	301.9	-1.105	0.848	-22.60	42.92
	$2 < T \le 3$	1.673	2.814	-22.54	54.16	-28.80	47.36	-1.581	12.14	-41.35	53.56
	$3 < T \le 4$	2.237	0.793	-8.539	21.84	-77.07	122.7	-2.482	37.97	-74.12	68.48
5%	$0.1 \le T \le 0.5$	-1.325	18.81	-94.07	-40.43	277.8					
	$0.5 < T \le 1$	-1.298	18.26	-83.81	-118.2	293.6					
	$1 < T \le 1.5$	3.441	-3.002	10.67	17.02	-40.21	61.66	-1.786	18.25	-28.95	44.21
	$1.5 < T \le 2$	18.00	10.10	-96.30	294.0	-378.2	435.5	-1.288	1.309	-22.59	43.85
	$2 < T \le 3$	1.484	2.776	-21.62	51.15	-21.54	40.17	-1.660	12.01	-41.45	54.26
	$3 < T \le 4$	2.250	0.400	-6.422	18.90	-76.87	124.3	-2.764	38.59	-74.43	69.76
10%	$0.1 \le T \le 0.5$	-1.303	18.65	-94.63	-39.88	277.8					
	$0.5 < T \le 1$	-1.496	20.53	-92.20	-134.6	305.0					
	$1 < T \le 1.5$	3.064	-2.537	8.716	17.71	-34.15	52.98	-1.553	20.51	-30.38	43.47
	$1.5 < T \le 2$	22.37	9.553	-98.18	320.0	-474.4	569.7	-1.319	-1.515	-20.63	44.13
	$2 < T \le 3$	1.587	2.731	-21.47	51.51	-24.66	44.48	-1.608	15.12	-43.21	54.59
	$3 < T \le 4$	2.272	0.118	-4.503	15.03	-77.04	127.7	-2.663	39.25	-75.04	69.84

inelastic deformation. Since EBSE is a rational approach for seismic evaluation taking into account the accumulated earthquake induced damage, there is a need to develop hysteretic energy spectrum equations overcoming some deficiencies and in particular complexities of the previous equations to be able to be applied in the code regulations. Accordingly, a new equivalent linear model has been represented, which is capable to predict hysteretic energy of nonlinear SDOF systems at different levels of ductility. Minimization of error has been developed through the concept of equivalent linearization, which resulted in equivalent damping and period as the representative parameters of the linear model. Two sets of ground motions based on the distance from fault rupture has been utilized,

referred to as the far- and near-field. The equivalent linear parameters determined in this study reflect the differences in the ground motion characteristics. For example, for a constant equivalent damping, the optimum equivalent period ratio is longer as calculated based on far-field records set comparing to the records set of near-field. This is expected because hysteric energy will be provided a larger contribution in input energy whenever the near-field earthquake records are considered and consequently period elongation occurs more quickly compare to far-field set of records. In addition, it is concluded that optimum equivalent period ratios increase with ductility for classes of initial period smaller than T_p, whereas for the other classes generally descending trend is observed. For a given value of ductility, it is observed that the ratio of equivalent to initial period is increased as equivalent damping increases while the minimum error corresponds to the larger values of equivalent damping. In this study, it is also investigated to see how period classes and post yield slope ratio can affect parameters of the new equivalent linear model.

The equivalent linear parameter equations developed in this methodology represent a significant improvement over the existing previous equations. The methodology has produced equivalent linear parameters, which are not dependent on response related parameters and, also records characteristics such as PGA, PGV, PGD or number of cycles. The equations are significantly more applicable specially to utilize in performance-based engineering.

References

Arroyo, D., and Ordaz, M. (2007), "On the estimation of hysteretic energy demands for SDOF systems", *Earthq. Eng. Struct. Dyn.*, **36**(15), 2365-2382. https://doi.org/10.1002/eqe.736.

ATC-40 (1996), *Seismic Evaluation and Retrofit of Concrete Building*, Applied Technology Council, Redwood City, California, U.S.A.

Browning, J., Warden, B., Matamoros, A. and Lepage, A. (2008), "Global and local seismic drift estimates for RC frames", *Eng. Struct.*, **30**(5), 1262-1271. https://doi.org/10.1016/j.engstruct.2007.07.003.

Cheng, Y., Lucchini, A. and Mollaioli, F. (2015), "Correlation of elastic input energy equivalent velocity spectral values", *Earthq. Struct.*, **8**(5), 957-976. http://dx.doi.org/10.12989/eas.2015.8.5.957.

D'Ambrisi, A. and Mezzi, M. (2015), "An energy-based approach for nonlinear static analysis of structures", *Bull. Earthq. Eng.*, **13**(5), 1513-1530. https://doi.org/10.1007/s10518-014-9673-2.

Decanini, L.D. and Mollaioli, F. (2001), "An energy-based methodology for the assessment of seismic demand", *Soil. Dyn. Earthq. Eng.*, **21**(2), 113-137. https://doi.org/10.1016/S0267-7261(00)00102-0.

Dindar, A.A., Yalçın, C., Yüksel, E., Özkaynak, H. and Büyüköztürk, O. (2015), "Development of earthquake energy demand spectra", *Earthq. Spectr.*, **31**(3), 1667-1689. https://doi.org/10.1193/011212EQS010M.

Enderami, S.A., Beheshti-Aval, S.B. and Saadeghvaziri, M.A. (2014), "New energy based approach to predict seismic demands of steel moment resisting frames subjected to near-fault ground motions", *Eng. Struct.*, **72**, 182-192. https://doi.org/10.1016/j.engstruct.2014.04.029.

Fajfar, P. and Vidic, T. (1994), "Consistent inelastic design spectra: Hysteretic and input energy", *Earthq. Eng. Struct. Dyn.*, **23**(5), 523-537. https://doi.org/10.1002/eqe.4290230505.

Fatahi, B., Tabatabaiefar, H.R. and Samali, B. (2014), "Soil-structure interaction vs. Site effect for seismic design of tall buildings on soft soil", *Geomech. Eng.*, **6**(3), 293-320. http://dx.doi.org/10.12989/gae.2014.6.3.293.

Fatahi, B., Tabatabaiefar, H.R. and Samali, B. (2011), *Performance Based Assessment of Dynamic Soil-Structure Interaction Effects on Seismic Response of Building Frames*, InGeo-Risk 2011: Risk Assessment and Management, 344-351.

FEMA P695 (2009), *Quantification of Building Seismic Performance Factors*, Applied Technology Council for the Federal Emergency Management Agency, Washington, U.S.A.

Gulkan, P. and Sozen, M.A. (1974). "Inelastic responses of reinforced concrete structure to earthquake motions", *J. Am. Concrete Inst.*, **71**(12), 604-610.

Guyader, A.C. and Iwan, W.D. (2006), "Determining equivalent linear parameters for use in a capacity spectrum method of analysis", *J. Struct. Eng.*, **132**(1), 59-67. https://doi.org/10.1061/(ASCE)0733-9445(2006)132:1(59).

Housner, G.W. (1956), "Limit design of structures to resist earthquakes", *Proceedings of the 1st WCEE*, Berkeley, California, U.S.A.

Iwan, W.D. (1980), "Estimating inelastic response spectra from elastic spectra", *Earthq. Eng. Struct. Dyn.*, **8**(4), 375-388. https://doi.org/10.1002/eqe.4290080407.

Kalkan, E. and Kunnath, S.K. (2007), "Effective cyclic energy as a measure of seismic demand", *J. Earthq. Eng.*, **11**(5), 725-751. https://doi.org/10.1080/13632460601033827.

Kowalsky, M.J. (1994), "Displacement-based design-a methodology for seismic design applied to RC bridge columns", M.Sc. Dissertation, University of California at San Diego, California, U.S.A.

Kunnath, S.K. and Chai, Y.H. (2004), "Cumulative damage-based inelastic cyclic demand spectrum", *Earthq. Eng. Struct. Dyn.*, **33**(4), 499-520. https://doi.org/10.1002/eqe.363.

Manfredi, G. (2001), "Evaluation of seismic energy demand", *Earthq. Eng. Struct. Dyn.*, **30**(4), 485-499. https://doi.org/10.1002/eqe.17.

Manoukas, G.E., Athanatopoulou, A.M. and Avramidis, I.E. (2014), "Multimode pushover analysis based on energy-equivalent SDOF systems", *Struct. Eng. Mech.*, **51**(4), 531-546. https://doi.org/10.12989/sem.2014.51.4.531.

Massumi, A. and Gholami, F. (2016), "The influence of seismic intensity parameters on structural damage of RC buildings using principal components analysis", *Appl. Math. Model.*, **40**(3), 2161-2176. https://doi.org/10.1016/j.apm.2015.09.043.

Mezgebo, M.G. (2015), "Estimation of earthquake input energy, hysteretic energy and its distribution in MDOF structures", Ph.D. Dissertation, Syracuse University, New York, U.S.A.

Molazadeh, M. and Saffari, H. (2018), "The effects of ground motion duration and pinching-degrading behavior on seismic response of SDOF systems", *Soil. Dyn. Earthq. Eng.*, **114**, 333-347. https://doi.org/10.1016/j.soildyn.2018.06.032.

Monavari, B. and Massumi, A. (2012), "Estimating displacement demand in reinforced concrete frames using some failure criteria", *Int. J. Adv. Struct. Eng.*, **4**(4), 1-6. https://doi.org/10.1186/2008-6695-4-4.

Oguzmert, M., and Lui, E.M. (2011), "Seismic design of inelastic structures using equivalent linear system parameters: Part 1-derivation and comparison", *IES J. Part A: Civil Struct. Eng.*, **4**(2), 89-102. https://doi.org/10.1080/19373260.2011.566009.

Otani, S., Hiraishi, H., Midorikawa, M. and Teshigawara, M. (2000), "New seismic design provisions in Japan", *Proceedings of the 2nd US-Japan Workshop on Performance-Based Earthquake Engineering Methodology for Reinforced Concrete Structures*, Sapporo, Hokkaido, Japan, September.

Priestley, M.J.N., Kowalsky, M.J., Ranzo, G. and Benzoni, G.

(1996), "Preliminary development of direct displacement-based design for multi-degree of freedom systems", *Proceedings of the 65th Annual SEAOC Convention*, Maui, Hawaii, U.S.A.

Riddell, R. and Garcia, J.E. (2001), "Hysteretic energy spectrum and damage control", *Earthq. Eng. Struct. Dyn.*, **30**(12), 1791-1816. https://doi.org/10.1002/eqe.93.

Samimifar, M. and Massumi, A. (2018), "Simplification and assessment of modal-based story damage index for reinforced concrete frames subjected to seismic excitations", *J. Earthq. Eng.*, **22**(3), 333-355. https://doi.org/10.1080/13632469.2016.1217803.

Su, L., Xiao, N. and Wang, Y. (2012), "A statistical approach to determine 2D optimal equivalent linear parameters with application to earthquake engineering", *Earthq. Eng. Eng. Vibr.*, **11**(3), 415-425. https://doi.org/10.1007/s11803-012-0131-3.

Sun, G., Gu, Q. and Fang, Y. (2017), "A simplified normalized cumulative hysteretic energy spectrum", *Earthq. Struct.*, **12**(2), 177-189. https://doi.org/10.12989/eas.2017.12.1.177.

Uang, C.M. and Bertero, V.V. (1990), "Evaluation of seismic energy in structures", *Earthq. Eng. Struct. Dyn.*, **19**(1), 77-90. https://doi.org/10.1002/eqe.4290190108.

Wang, F., Ke, K., Zhang, H. and Yam, M.C. (2018), "Constant-ductility-based energy factor demands of oscillators with modified Clough hysteretic model", *Soil. Dyn. Earthq. Eng.*, **115**, 36-40. https://doi.org/10.1016/j.soildyn.2018.08.014.

Yaghmaei-Sabegh, S., Neekmanesh, S. and Lumantarna, E. (2014), "Nonlinear response estimates of RC frames using linear analysis of SDOF systems", *Earthq. Eng. Struct. Dyn.*, **43**(5), 769-790. https://doi.org/10.1002/eqe.2371.

CC